Is the coefficient of eddy potential vorticity diffusion positive?

Part1: barotropic zonal channel.

V.O. Ivchenko[1]

V.B. Zalesny[2]

B.Sinha[3]

[1] University of Southampton,

National Oceanography Centre, Southampton UK (retired)

[2] Institute of Numerical Mathematics, Moscow, Russia

[3] National Oceanography Centre, Southampton UK

corresponding author, Vladimir Ivchenko, voi@noc.soton.ac.uk

ABSTRACT

The question of whether the coefficient of diffusivity of potential vorticity by mesoscale eddies is positive is studied for a zonally reentrant barotropic channel using the quasi-geostrophic approach. The topography is limited to the first mode in the meridional direction but is unlimited in the zonal direction. We derive an analytic solution for the stationary (time-independent) solution. New terms associated with parameterized eddy fluxes of potential vorticity appear both in the equations for the mean zonal momentum balance, and the kinetic energy balance. These terms are linked with the topographic form stress exerted by parameterized eddies. It is demonstrated that in regimes with zonal flow (analogous to the Antarctic Circumpolar Current), the coefficient of eddy potential vorticity diffusivity must be positive.

1. Introduction

Mesoscale eddies are a very important element of the global ocean since they usually account for the main peak in the kinetic energy spectrum (Kamenkovich *et al.* 1986; McWilliams 2008; Wunsch and Stammer, 1995). This means that ocean models have to either resolve or parameterize them. To resolve the mesoscale, horizontal grids in models must be much smaller than the internal Rossby radii of deformation. Improvements in computing capability (both memory and speed) allow us to run global models with high resolution. However weak stratification in the polar regions and the associated small internal Rossby radii (2-3km) still preclude adequate resolution to explicitly resolve eddies in these areas. Another significant problem is the appearance of strong internal variability with increasing resolution. Small disturbances can results in energetic noise, which can only be removed by averaging over ensembles of numerical experiments; for example the UK Met Office routinely runs ensembles of 10 members for decadal predictions and 42 members for seasonal prediction (Smith *et al.* 2007). Rather than employing an ensemble of high resolution model simulations to realistically represent eddies and their effects on the mean flow, another approach is to utilize lower resolution models and include a parameterization of the important effects of the eddies on the large scale circulation. It is very likely that mesoscale eddy parameterization "will be needed for some decades into the future" (Bachman and Fox-Kemper 2013).

Parameterization of mesoscale eddies is important not only for practical reasons (reduced computational expense), but also for theoretical reasons: a physically correct parameterization allows us to better understand the dynamics of eddy-eddy and eddy-mean flow interactions, i.e. fundamental parts of geophysical fluid dynamics. There have been many studies devoted to this problem, for example: Green (1970); Welander (1973); Marshall (1981); Ivchenko (1984), Gent and McWilliams (1990); Ivchenko *et al.* (1997); Killworth (1997); Treguier *et al.* (1997); Olbers *et al.* (2000); Wardle and Marshall (2000); Olbers (2005); Eden (2010); Marshall and Adcroft (2010); Ringler and Gent (2011); Marshall *et al.* (2012);

Ivchenko *et al.* (2013), (2014(a)), (2014(b)); and many others.

The most popular approach to parameterization is use of the so-called diffusive parameterization, i.e proportionality of eddy fluxes of a property A to its mean gradient:

$$\langle A' v_j' \rangle = -K \frac{\partial \langle A \rangle}{\partial x_j} \ , \tag{1}$$

where v_j is the velocity component, x_j is a spatial coordinate, the $\langle \, . \, \rangle$ denotes some averaging, and primes mark eddy components (deviations from that average). K is the coefficient of transfer, in principle a tensor, but for simplicity here assumed to be a scalar. The diffusive parameterization should only be applied for a conservative property.

There has been much interest in applying a diffusive parameterization to potential vorticity (PV) (Green 1970; Welander 1973; Marshall 1981). Importantly, if we use a diffusive parameterization of potential vorticity we do not need to separately parameterize eddy momentum and buoyancy fluxes, because they are already included in the eddy flux of potential vorticity. While the parameterization in terms of PV is well suited to approximations such as the quasigeostrophic formulation, primitive equation models widely used today are formulated in terms of the momentum equations and do not lend themselves as easily to a diffusive parameterization of PV.

Using a diffusive closure of eddy PV fluxes requires an integral constraint for the momentum budget known as the theorem of Bretherton to be introduced (Bretherton 1966; McWilliams *et al.* 1978; Marshall 1981) (see Section 3). Some studies (Marshall 1981; Ivchenko 1984; Ivchenko *et al.* 1997; 2013; 2014a,b; Olbers *et al.* 2000) satisfy the momentum constraint by a suitable choice of diffusivity coefficient, and others by inclusion of a so-called "gauge" term (Eden 2010).

McWilliams *et al.*(1978) and McWilliams and Chow (1981) demonstrated sharpening of zonal flow by PV mixing in an eddy resolving quasigeostrophic zonal channel model. It was further demonstrated that using a diffusive parameterization of quasigeostrophic PV (QGPV) in a zonal channel can result in sharper and stronger currents (Ivchenko 1984; Ivchenko *et al.* 1997; 2014b), provided a spatially variable positive diffusion coefficient is

specified, with local minima in regions occupied by jets. Dritschel and McIntyre (2008) and Wood and McIntyre (2010) also performed theoretical studies of sharpening of zonal flows by PV diffusion.

Application of a diffusive parameterization of PV in a zonal reentrant channel (with application to the Antarctic Circumpolar Current, ACC) has been studied in many papers both for domains with a flat bottom and domains with bottom topography included, but only for the zonally averaged case (Marshall 1981; Ivchenko 1984; Ivchenko *et al.* 1997; 2013; 2014a, b). Introduction of bottom topography creates a number of difficult complications (see Constantinou and Young, 2017).

There are two major questions associated with application of a diffusive parameterization of PV in the presence of bottom topography:

1) Is the eddy PV diffusivity coefficient K guaranteed to be positive? K varies in space and time. Probably its local value in some locations could occasionally be negative. However, can we be sure that the mean (averaged) value of K is positive? Rhines and Young (1982) suggested that the eddy flux of PV is downgradient (i.e. positive eddy PV diffusivity) in an integral sense. There are not many analytical works that constrain the sign of PV diffusion. Abernathey *et al.* (2013) made an analysis based on a primitive equation model for a circumpolar channel. However, following Treguier *et al.* (1997) they calculated certain quasigeostrophic quantities, such as QGPV flux, background QGPV gradient and corresponding diffusivity, using zonal averaging. The QGPV diffusivity is positive nearly everywhere, except near the surface, where the QG approximation is invalid. Birner *et al.* (2013), on the other hand, reveal a localized region of significant up-gradient eddy PV fluxes on the poleward side of the subtropical free atmospheric jet core during the winter and spring seasons of both hemispheres. However, Birner *et al.* (2013) have noted that the net PV fluxes are down-gradient when averaged over both the equatorward and poleward flanks of the jet.

In this study an analytical solution is provided which supports PV diffusivity being

positive (in a domain-averaged sense). The assumption of a spatially constant eddy PV diffusivity is clearly unrealistic, however, it leads a mathematically tractable problem and the solution provides insights which will remain applicable in the more general case.

2) How does one deal with the rotational (non divergent) part of eddy PV flux? Eddy fluxes of PV comprise a rotational component, and a divergent component: any vector $\mathbf{E}$ can be separated into divergent $\mathbf{E_{div}}$ and rotational $\mathbf{E_{rot}}$ parts (see next section).

The rotational component of the eddy flux of potential vorticity is likely to be substantial for a zonal channel with bottom topography (Sinha 1993). However the rotational part does not directly influence the flow, because the divergence of the eddy flux appears in the PV equation and so the contribution of the rotational component is zero. The rotational part can, however, influence the flow by influencing the coefficient K via the equation of eddy potential enstrophy (see Section 2).

How can we determine the sign of K for eddy diffusion of PV? One suggestion would be to use the results of eddy resolving experiments with oceanic GCMs. We can calculate $\langle\, Q'v'_j \,\rangle$ (Q is PV), and $\partial\langle\, Q \,\rangle/\partial\, x_j$ directly from model simulations, and then determine

$$K = -\frac{\langle\, Q'v'_j \,\rangle}{\frac{\partial <Q>}{\partial\, x_j}} \quad . \tag{2}$$

However, as already noted, the rotational part of $\langle\, Q'v'_j \,\rangle$ must be excluded from this calculation. A lack of inherited boundary condition makes separation of eddy fluxes of PV into divergent and rotational components for a finite domain with non-periodic boundary conditions non-unique, as shown by Fox-Kemper *et al.* (2003).

Separation of the eddy PV flux into divergent and rotational components requires a specific boundary condition. Maddison *et al.* (2015) defined the divergent component of the PV flux by introducing a streamfunction tendency ("force function"). This is equivalent to a zero tangential component boundary condition (zero normal flux), and hence is not completely general. Mak *et al.* (2016) introduced a new method for diagnosing eddy diffusivity in a gauge-invariant fashion, which is independent of rotational flux components. This was achieved by seeking to match diagnosed and parameterized eddy force functions through an

optimisation procedure. The method was applied to a multi-layer QG ocean gyre experiment and it was demonstrated that the mean PV diffusivity over the horizontal domain is positive, however, robust locally negative diffusivity takes place even in the absence of rotational fluxes.

An alternative possibility is to determine the sign of the coefficient theoretically. In this study we derive an analytical solution and construct an expression for kinetic energy, integrated over the whole domain and use physical constraints on kinetic energy to demonstrate that the sign of K, interpreted as a domain-averaged PV diffusivity, must be positive. This is the first time that an analytical solution using a diffusive parameterization of PV has been derived for a barotropic quasigeostrophic zonal channel flow above zonally varying bottom topography. It is not, however, our intention to compare the relative merits of alternative eddy parameterizations.

The remainder of this paper is organised as follows. In Section 2 we present the basic equations for quasigeostrophic barotropic flow and equations for a zonal channel geometry with bottom topography. In Section 3 we formulate the generalized theorem of Bretherton. In Section 4 we demonstrate an analytical solution for zonal flow, construct an expression for kinetic energy and present results of our calculations for different types of topography. Section 5 consists of discussion and conclusions.

2. Equations for zonal channel geometry including eddy parameterization

The equation for barotropic quasigeostrophic vorticity can be written as:

$$\frac{\partial q}{\partial t} + J(\Psi, q) = T + F_B + F_H \ , \tag{3}$$

where q and Ψ are the quasigeostrophic potential vorticity (QGPV) and streamfunction, respectively. Velocity $\mathbf{v} = (u, v)$ is related to the streamfunction by $u = -\frac{\partial}{\partial y}\Psi$ and $v = \frac{\partial}{\partial x}\Psi$,

where u and v are the velocity components in the zonal (x) and meridional (y) directions. $J(A,B)$ is the Jacobian operator: $J(A,B) = -\frac{\partial A}{\partial y}\frac{\partial B}{\partial x} + \frac{\partial A}{\partial x}\frac{\partial B}{\partial y}$. T, F_B, and F_H are the external forcing (wind stress), bottom and horizontal friction, respectively.

The QGPV, q, in barotropic flow represents the sum of relative vorticity, planetary vorticity and the topographic term given by:

$$q = \nabla^2\Psi + f + \frac{f_0}{H}B \ , \tag{4}$$

where Coriolis parameter $f = f_0 + \beta\, y$. f_0 and β denote its value at a reference latitude and its meridional gradient respectively. B is the deviation of bottom topography from a constant depth H.

Bottom topography substantially complicates the dynamics. The streamfunction exhibits non-zonal meanders near topographic obstacles (McWilliams *et al.*, 1978) and therefore it is necessary to perform spatial averaging not for the whole zonal length, but for only part of it. The averaged equations depend on both zonal and meridional directions, which creates much more mathematical complexity compared to the fully zonally averaged case, but they remain analytically tractable as we will demonstrate.

In order to understand eddy dynamics it is important to consider the equation for quasi-geostrophic eddy potential enstrophy (QGEPE). To derive the QGEPE equation, we define a time- and partial zonal average of an arbitrary variable, denoted by an overbar, $\overline{A}$ and a deviation from this average, denoted by a superscript prime $A' = A - \overline{A}$:

$$\overline{A(x,t)} = \frac{1}{2\delta_x T}\int_t^{t+T}\int_{x-\delta_x}^{x+\delta_x} A(x',t')dx'\,dt' \ , \tag{5}$$

where δ_x is the average scale for zonal coordinate, and T is the averaging time. Note, that the partial zonal and time average is a more appropriate type of average for the zonal channel domain with variable topography than a time only average, since bottom topography being time-independent cannot contribute to the eddy topographic form stress in the case of a time average (see Section 3).

We average equation (3), subtract the resulting equation from (3), multiply by q' and average once again to obtain:

$$\frac{1}{2}\frac{\overline{\partial\, q'^2}}{\partial\, t} = 0 = -\frac{1}{2}div(\overline{\mathbf{v}}\overline{q'^2}) - \overline{\mathbf{v}'\, q'}\cdot\ \nabla\overline{q} - \frac{1}{2}div(\overline{\mathbf{v}'\, q'^2}) + \overline{T'\, q'} + \overline{F'_B\, q'} + \overline{F'_H\, q'}\ \ . \qquad (6)$$

Equation (6) is a well known equation for quasigeostrophic eddy potential vorticity QGEPE (see e.g. Vallis 2006). The terms on the RHS of equation (6) represent redistribution by the mean flow, generation, redistribution by eddies, input from external sources and dissipation by bottom and horizontal friction, of QGEPE, respectively.

If we now specify the domain as a zonal reentrant channel, and integrate (6) over the whole domain S, then the terms responsible for redistribution (i.e. the first and the third terms on the RHS) drop out because of boundary conditions on the solid walls and periodicity. A similar equation was derived by Constantinou and Young (2017). We assume that the external forcing is stationary ($T' = 0$), and therefore the 4th term on the RHS is zero, which leads to:

$$\int_{(S)} \frac{1}{2}\frac{\overline{\partial\, q'^2}}{\partial\, t} dS = 0 = -\int_{(S)} \overline{\mathbf{v}'\, q'}\cdot\ \nabla\overline{q} dS + \int_{(S)} (\overline{F'_B\, q'} + \overline{F'_H\, q'}) dS\ \ . \qquad (7)$$

Equation (7) represents the balance between the generation of the QGEPE (the first term on the RHS) and dissipation by bottom and horizontal friction. The dissipation terms measure the integral loss of enstrophy, therefore the integral of the generation should be positive. Numerical experiments with eddy resolving models demonstrate that the generation term locally takes both signs (Sinha 1993; J-O. Wolff, personal communication). However the integral over the domain must be positive.

The eddy flux $\overline{\mathbf{v}'\, q'}$ comprises two parts: the divergent flux $\mathbf{E_{div}}$ and rotational flux $\mathbf{E_{rot}}$:

$$\overline{\mathbf{v}'\, q'} = \mathbf{E_{div}} + \mathbf{E_{rot}}\ \ , \qquad (8)$$

where $curl_z(\mathbf{E_{div}}) = 0$, $div(\mathbf{E_{rot}}) = 0$, $curl_z\mathbf{E}_{div} = \frac{\partial \mathbf{E}_{div}|_y}{\partial\, x} - \frac{\partial \mathbf{E}_{div}|_x}{\partial\, y}$.

The traditional diffusive parameterization of QGPV can be written as:

$$\overline{\mathbf{v}'\, q'} = -k\nabla\overline{q}\ \ , \qquad (9)$$

and the term representing generation of QGEPE in equations (6,7) is:

$$\overline{\mathbf{v}'\, q'} \cdot \nabla \overline{q} = -k |\nabla \overline{q}|^2 \ , \tag{10}$$

where k is the coefficient of eddy diffusivity of QGPV.

The equation for mean QGPV (3) for the stationary (time-independent case) takes the following form :

$$\overline{u} \frac{\partial \overline{q}}{\partial x} + \overline{v} \frac{\partial \overline{q}}{\partial y} + \frac{\partial \overline{u'q'}}{\partial x} + \frac{\partial \overline{v'q'}}{\partial y} = \frac{1}{H} curl_z \overline{\boldsymbol{\tau}} - \epsilon \, curl_z \overline{\mathbf{v}} \ . \tag{11}$$

We specify QGPV input due to surface wind stress in the traditional manner: $T = \frac{1}{H} curl_z \overline{\boldsymbol{\tau}}$, where $\boldsymbol{\tau}$ represents tangential wind stress divided by the water density, and $F_B = -\epsilon \, curl_z \overline{\mathbf{v}}$, bottom friction, where ϵ is a coefficient of bottom friction. Horizontal friction is disregarded.

Using (9), equation (11) becomes:

$$\overline{u} \frac{\partial \overline{q}}{\partial x} + \overline{v} \frac{\partial \overline{q}}{\partial y} - \frac{\partial}{\partial x} k \frac{\partial \overline{q}}{\partial x} - \frac{\partial}{\partial y} k \frac{\partial \overline{q}}{\partial y} = \frac{1}{H} curl_z \overline{\boldsymbol{\tau}} - \epsilon \, curl_z \overline{\mathbf{v}} \ . \tag{12}$$

We proceed to solve (12) by expanding each of the variables into a Fourier series. We assume that the bottom topography has meridional length-scale comparable with the width of the channel L and retain only the first term in the Fourier decomposition of topography in the meridional direction. In the zonal direction we allow a variety of length-scales for bottom topography, both large and small scales and impose no limit to the number of terms in the Fourier series. Such detailed representation in the zonal direction is important for zonal flows, because it allows better representation of the non-viscous bottom form stress, which is important for balancing the external forcing (wind stress) and results in a substantial decrease of the zonal transport, compared with the flat bottom case (Munk and Palmen 1951; McWilliams *et al.* 1978; Wolff *et al.* 1991).

We assume no mass flux through the solid walls:

$$\overline{v}|_{y=0,L} = 0 \ . \tag{13}$$

We also assume no QGPV flux through the walls:

$$\overline{v'q'}|_{y=0,L} = -k \frac{\partial \overline{q}}{\partial y} = 0 \ . \tag{14}$$

Condition (14) can only be satisfied if k is zero on the solid walls, because of the presence of the planetary vorticity gradient β in the expression for the meridional gradient of QGPV i.e. on the boundaries $\partial\overline{q}/\partial\, y$ cannot be zero therefore k must be zero. Hence, we specify the following form of the coefficient k:

$$k = k_0\{1 + e^{(-L/\Delta)} - e^{(-y/\Delta)} - e^{(y-L)/\Delta)}\} \ , \tag{15}$$

where $\Delta \ll L$ and k_0 is a constant. k is almost constant in the domain, but quickly drops to zero on the side walls (see Fig. 1). The difference between k and k_0 at any point of the domain will be small by choosing Δ to be small enough, except on the solid boundaries, where $k = 0$.

3. Generalized theorem of Bretherton

In a zonal channel with a flat bottom the total (domain averaged) meridional eddy fluxes of QGPV must be zero, to satisfy the mean zonal momentum budget (Bretherton 1966). This statement, known as the theorem of Bretherton (McWilliams, *et al.* 1978), provides an integral constraint for coefficients of QGPV diffusivity (Marshall 1981, Ivchenko 1984). In a zonal channel with variable bottom topography this statement can be generalized using zonal and time averaging (Ivchenko *et al.* 1987b; Ivchenko *et al.* 2013, 2014a), which allows us to include an important topographic form stress in the mean zonal momentum balance. In this study we find a solution depending on both meridional and zonal coordinates and therefore use partial zonal and time averages (5) . Let us first calculate the eddy QGPV flux by multiplying q (see (4)) by v', taking an average and integrating over the whole basin:

$$\int_0^L \int_0^{L_x} \overline{v'q} dx\, dy = \int_0^L \int_0^{L_x} \{\overline{v'(\frac{\partial\, v}{\partial\, x} - \frac{\partial\, u}{\partial\, y})} + f\overline{v'} + \frac{f_0}{H}\overline{v'B}\} dx\, dy \ , \tag{16}$$

where L_x is the zonal length of the channel. The first term in the RHS of (16) can be transformed, using the continuity equation:

$$\int_0^L \int_0^{L_x} \overline{v'(\frac{\partial\, v}{\partial\, x} - \frac{\partial\, u}{\partial\, y})} dx\, dy = \int_0^L \int_0^{L_x} (\frac{1}{2}\frac{\partial\, \overline{v'^2}}{\partial\, x} - \frac{\partial\, \overline{u'\, v'}}{\partial\, y} - \frac{1}{2}\frac{\partial\, \overline{u'^2}}{\partial\, x}) dx\, dy \ . \tag{17}$$

The first and the third terms in the RHS of (17) drop to zero because of periodicity, and the second term drops to zero because there is no flux through the solid walls. It is obvious that the second term in the RHS of (16) is zero, so using $\overline{v'q} = \overline{v'q'}$ equation (16) can be written as:

$$\int_0^L \int_0^{L_x} \overline{v'q'} dx\, dy = \int_0^L \int_0^{L_x} \frac{f_0}{H} \overline{v'B'} dx\, dy \quad . \tag{18}$$

This means that redistribution of QGPV by eddies (LHS) is balanced by topographic form stress (RHS), exerted by eddies.

If we introduce a diffusive parameterization (9) together with the expression for k (15) into the LHS of (18) we obtain:

$$\int_0^L \int_0^{L_x} \overline{v'q'} dx\, dy = -\beta\, k_0 L_x L \{1 + e^{(-L/\Delta)} - \frac{2\Delta(1 - e^{(-L/\Delta)})}{L}\} \quad . \tag{19}$$

The expression in curly brackets is close to unity. Therefore (18) becomes:

$$-\beta\, k_0 = \frac{f_0}{H} \frac{1}{L_x L} \int_0^L \int_0^{L_x} \overline{v'B'} dx\, dy \quad . \tag{20}$$

The $\beta\, k_0$ term appeared in studies by Welander (1973), Killworth (1997), Eden (2010) and many others. Equation (20) provides a clear physical explanation of this term: eddy topographic form stress is exerted by parameterized eddies. Note that using only time averaging without partial zonal averaging would lead to the eddy flux associated with the topographic part of the QGPV dropping to zero (bottom topography is time independent, hence the RHS of (20) is zero) and this would imply that the coefficient k_0 has to be zero.

4. Analytical solution for zonal flow

a. Model setup

We now assume that the solution for equation (12) consists of a constant zonal flow with (unknown) velocity U and streamfunction Φ multiplied by the first meridional Fourier mode:

$$\overline{\Psi} = -Uy + \Phi(x) \sin(\pi\, y/L) \quad . \tag{21}$$

We follow Charney *et al.* (1981) who used a similar technique for an atmospheric flow in a zonal channel. We represent the topographic term B in the form:

$$B = h(x)\sin(\pi\, y/L) \ . \tag{22}$$

The net zonal transport across the channel depends only on U, because $\Phi(x)\sin(\frac{\pi\, y}{L})$ does not affect the net transport, although it does affect the zonal velocity locally because of topography and diffusion of the QGPV. We specify the surface windstress, $\boldsymbol{\tau} = (\tau_x, \tau_y)$, with $\tau_y = 0$, and let the zonal component of wind stress be proportional to the sine of latitude with the maximum value in the centre of the channel and zero on the walls, i.e. $\tau_x = \tau_0 \sin(\frac{\pi\, y}{L})$.

Using (21-22) the velocity and the gradient of potential vorticity can be easily calculated. So, equation (12) after transformation can be rewritten in this form:

$$\sin(\pi\, y/L)\{U\Phi_{xxx} - U\frac{\pi^2}{L^2}\Phi_x + \beta\Phi_x + \frac{f_0}{H}\,U h_x$$

$$-k\Phi_{xxxx} + k\frac{\pi^2}{L^2}\Phi_{xx} - k\frac{f_0}{H}h_{xx}\} + \frac{\partial}{\partial\, y}(\overline{v'\, q'})$$

$$+\sin(\pi\, y/L)\cos(\pi\, y/L)\{-\frac{\pi}{L}\Phi\Phi_{xxx} - (\frac{\pi}{L})\frac{f_0}{H}(\Phi h_x - \Phi_x\, h)$$

$$+\frac{\pi}{L}\Phi_x\Phi_{xx}\} = -\frac{\tau_0\pi}{HL}\cos(\pi\, y/L) - \sin(\pi\, y/L)[\epsilon\Phi_{xx} - \epsilon\,(\frac{\pi}{L})^2\Phi] \ . \tag{23}$$

Subscripts x (Φ_x, h_x and so on) mark zonal derivatives, and the number of subscripts correspond to the derivative order: $\Phi_x = \partial\,\Phi/\partial\, x$, $\Phi_{xx} = \partial^2\,\Phi/\partial\, x^2$, and so on. In equation (23) the term of meridional gradient of the meridional flux of eddy QGPV is retained without transformation since it simplifies after a meridional integration which we carry out in Section 4b.

b. Momentum balance

In order to simplify the QGPV equation and remove the y-dependence we integrate (23) meridionally between 0 and L, resulting in

$$U(\Phi_{xxx} - \frac{\pi^2}{L^2}\Phi_x) + U\frac{f_0}{H}h_x + \Phi_x\beta - k_0[\Phi_{xxxx} - \frac{\pi^2}{L^2}\Phi_{xx} + \frac{f_0}{H}h_{xx}]$$

$$\{1 - \frac{\pi^2\Delta^2(1+e^{(-L/\Delta)})}{(L^2+\pi^2\Delta^2)}\} + \epsilon\Phi_{xx} - \epsilon(\frac{\pi}{L})^2\Phi = 0 \ . \tag{24}$$

To derive this equation we assume that the eddy flux through the solid walls is zero $\overline{v'\,q'} = 0$ (boundary condition (14)). We also make use of the property that terms proportional to $\sin(\frac{\pi\,y}{L})\cos(\frac{\pi\,y}{L})$ integrate to zero.

We can obtain a further useful relationship by returning to (23), multiplying by $\cos(\frac{\pi\,y}{L})$ and integrating meridionally between the solid boundaries. There is an important term $\int_0^L \cos(\pi\,y/L)\frac{\partial}{\partial\,y}(\overline{v'\,q'})dy$, which after substitution of (9) and (15), becomes:

$$\int_0^L \cos(\pi\,y/L)\frac{\partial}{\partial\,y}k\frac{\partial\overline{q}}{\partial\,y}dy = 2\beta\,k_0\{1 + e^{(-L/\Delta)} - \frac{\pi^2\Delta^2(1+e^{(-L/\Delta)})}{(L^2+\pi^2\Delta^2)}\} \ . \tag{25}$$

So equation (23) multiplied by $\cos(\frac{\pi\,y}{L})$ and integrated meridionally yields:

$$\Phi\Phi_{xxx} - \Phi_x\Phi_{xx} + \frac{f_0}{H}(\Phi h_x - \Phi_x\,h) + 3\beta\,k_0\{1 + e^{(-L/\Delta)}$$

$$-\frac{\pi^2\Delta^2(1+e^{(-L/\Delta)})}{(L^2+\pi^2\Delta^2)}\} = \frac{3\tau_0\pi}{4H}. \tag{26}$$

Note that because $\Delta \ll L$ the expressions in the curly brackets in (24-26) are very close to unity, so we approximate them as unity with negligible error.

We integrate (26) with respect to x between 0 and L_x to eliminate the zonal dependence and elucidate the zonal momentum balance:

$$\int_0^{L_x}\{\Phi\Phi_{xxx} - \Phi_x\Phi_{xx} + \frac{f_0}{H}(\Phi h_x - \Phi_x\,h)\}dx + 3\beta\,k_0L_x = \frac{3L_x\tau_0\pi}{4H} \ . \tag{27}$$

It is easy to show that

$$\int_0^{L_x}(\Phi\Phi_{xxx} - \Phi_x\Phi_{xx})dx = 0 \ , \tag{28}$$

because of the periodicity of the channel. Also,

$$\int_0^{L_x} (\Phi h_x) dx = -\int_0^{L_x} (\Phi_x \, h) dx \ . \tag{29}$$

Thus equation (27) can be rewritten as:

$$\frac{3 L_x \tau_0 \pi}{8} = f_0 \int_0^{L_x} (\Phi h_x) dx + \frac{3\beta \, k_0 L_x H}{2} \ . \tag{30}$$

Equation (30) describes the stationary momentum balance. On the LHS there is a contribution from wind stress. The first term on the RHS, i.e. $f_0 \int_0^{L_x} \Phi h_x \, dx$ is the topographic form stress exerted by the mean flow, since it is an integral of the product of a pressure (equal to streamfunction times Coriolis parameter f_0) and the zonal gradient of bottom topography. The second term on the RHS is a topographic form stress exerted by unresolved parameterized eddies on the bottom topography (see (20)).

c. Energy balance

We form the energy power integral by multiplying the y-integrated QGPV equation (24) with $\Phi(x)$ and integrate over x. After some manipulation we obtain:

$$U \frac{f_0}{H} \int_0^{L_x} (\Phi h_x) dx - k_0 \int_0^{L_x} (\Phi_{xx})^2 dx - k_0 \frac{\pi^2}{L^2} \int_0^{L_x} (\Phi_x)^2 dx + k_0 \frac{f_0}{H} \int_0^{L_x} \Phi_x h_x \, dx$$

$$-\epsilon \int_0^{L_x} (\Phi_x)^2 dx - \epsilon \frac{\pi^2}{L^2} \int_0^{L_x} (\Phi)^2 dx = 0 \ . \tag{31}$$

Substitution of (30) into (31) after transformation yields an equation of balance of kinetic energy of the "perturbed" flow $E = E_U + E_V$, where

$$E_U = \frac{1}{L_x L} \int_0^{L_x} \int_0^{L} \frac{(\overline{u} - U)^2}{2} dx dy \ , \tag{32}$$

$$E_V = \frac{1}{L_x L} \int_0^{L_x} \int_0^{L} \frac{\overline{v}^2}{2} dx dy \ . \tag{33}$$

For a steady-state, the kinetic energy balance equation of the perturbed flow can be written as:

$$\{E,\tau\} = \{E,k\} + \{E,h\} + \{E,\epsilon\} + \{E,\beta\} \quad . \tag{34}$$

The terms in (34) are as follows:

$$\{E,\tau\} = \frac{3\pi}{8H} U\tau_0 \tag{35}$$

represents generation of kinetic energy by wind stress;

$$\{E,k\} = \frac{k_0}{L_x}\int_0^{L_x}[(\Phi_{xx})^2 + \frac{\pi^2}{L^2}(\Phi_x)^2]dx > 0, \;\; (if \;\; k_0 > 0) \tag{36}$$

represents dissipation of energy by mixing of QGPV; and

$$\{E,h\} = -\frac{k_0}{L_x}\int_0^{L_x}[\frac{f_0}{H}\Phi_x h_x]dx > 0 \tag{37}$$

represents dissipation by QGPV mixing linked with bottom topography, and is positive because of conservation of QGPV. In the mainly eastward flow there is an equatorward (i.e. $\Phi_x > 0$) deflection if the motion is uphill ($h_x > 0$), and a poleward (i.e. $\Phi_x < 0$) deflection if the motion is downhill ($h_x < 0$). So, $-\frac{f_0}{H}\int_0^{L_x}\Phi_x h_x\,dx > 0$, since the Coriolis parameter is negative in the Southern Hemisphere. Note that the sign of this term is positive in the Northern Hemisphere as well, since not only is the Coriolis parameter of opposite sign, but the "equatorward/poleward" motions, are also reversed. The term

$$\{E,\epsilon\} = +\frac{\epsilon}{L_x}\int_0^{L_x}[(\Phi_x)^2 + \frac{\pi^2}{L^2}(\Phi)^2]dx > 0 \tag{38}$$

represents dissipation by bottom friction. The last term,

$$\{E,\beta\} = \frac{3Uk_0\beta}{2} > 0(if \;\; k_0 > 0), \tag{39}$$

is proportional to U, k_0 and β, and using (20) could be rewritten as

$$\{E,\beta\} = -\frac{3}{2}U\frac{f_0}{H}\frac{1}{L_x L}\int_0^{L}\int_0^{L_x}\overline{v'B'}dx\,dy \;\; , \tag{40}$$

and is a sink of kinetic energy due to topographic form stress exerted by parameterized eddies. A conceptually similar term was introduced by Carnevale and Frederiksen (1987) in their study of periodic flow on a β-plane. They consider how best to model the interaction of "small" scale (synoptic) flow features with large or basin scale features. Carnevale and Frederiksen (1987) emphasize the role of the integral invariants. They demonstrated that the rate of change of energy in the "small scales" is given by a term similar to the RHS of (40) (see the RHS of eq.(5.5) of the paper by Carnevale and Frederiksen 1987).

The three terms $\{E,k\}$, $\{E,h\}$ and $\{E,\beta\}$ are proportional to k_0 and represent dissipation of energy only if $k_0 > 0$. If $k_0 < 0$ all these terms are physically incorrect.

d. Analytical solution

To obtain an analytical solution let us write Φ, and topography $h(x)$ as Fourier series:

$$\Phi = \sum_n a_n \cos(\frac{2n\pi\, x}{L_x}) + \sum_n b_n \sin(\frac{2n\pi\, x}{L_x}) \ , \tag{41}$$

$$h = \sum_n c_n \cos(\frac{2n\pi\, x}{L_x}) + \sum_n d_n \sin(\frac{2n\pi\, x}{L_x}) \ , \tag{42}$$

where a_n and b_n are unknown constants, and c_n and d_n are constants relating to the prescribed topography. n is the index of each mode used in the Fourier expansion.

Substituting (41) and (42) in the meridionally integrated QGPV equation (24) and equating coefficients of $\sin(\frac{2n\pi\, x}{L_x})$ and $\cos(\frac{2n\pi\, x}{L_x})$ results in two equations:

$$a_n[UM^{(n)} - \beta\frac{2\pi}{L_x}\, n] - b_n N^{(n)} - c_n\, U\frac{f_0}{H}\frac{2\pi}{L_x}\, n + d_n\, k_0\frac{f_0}{H}(\frac{2\pi}{L_x})^2\, n^2 = 0 \ , \tag{43}$$

$$-a_n N^{(n)} + b_n[-UM^{(n)} + \beta\frac{2\pi}{L_x}\, n] + c_n\, k_0\frac{f_0}{H}(\frac{2\pi}{L_x})^2\, n^2 + d_n\, U\frac{f_0}{H}\frac{2\pi}{L_x}\, n = 0 \ , \tag{44}$$

where

$$M^{(n)} = (\frac{2\pi}{L_x})^3 n^3 + \frac{2\pi^3}{L^2 L_x} n \ , \tag{45}$$

330

$$N^{(n)} = k_0(\frac{2\pi}{L_x})^4 n^4 + k_0 \frac{4\pi^4}{L^2 L_x^2} n^2 + \epsilon\,(\frac{2\pi}{L_x})^2 n^2 + \epsilon(\frac{\pi}{L})^2 \quad . \tag{46}$$

331 Solution of the two algebraic equations (43) and (44) yields:

$$a_n = \frac{S_0^{(n)} + U S_1^{(n)} + U^2 S_2^{(n)}}{R_0^{(n)} + U R_1^{(n)} + U^2 R_2^{(n)}} \quad , \tag{47}$$

332

$$b_n = \frac{1}{N^{(n)}}\{\frac{U M^{(n)}[S_0^{(n)} + U S_1^{(n)} + U^2 S_2^{(n)}]}{R_0^{(n)} + U R_1^{(n)} + U^2 R_2^{(n)}} - \frac{\beta \frac{2\pi}{L_x}\, n[S_0^{(n)} + U S_1^{(n)} + U^2 S_2^{(n)}]}{R_0^{(n)} + U R_1^{(n)} + U^2 R_2^{(n)}}$$

333

$$-U c_n \frac{f_0}{H}\frac{2\pi}{L_x}\, n + d_n\, k_0 \frac{f_0}{H}(\frac{2\pi}{L_x})^2\, n^2\} \quad . \tag{48}$$

334 New parameters $R_0^{(n)}$, $R_1^{(n)}$, $R_2^{(n)}$, $S_0^{(n)}$, $S_1^{(n)}$, $S_2^{(n)}$, have been introduced. Their values can be
335 seen in the Appendix.

336 Coefficients a_n and b_n in expressions (47) and (48) still contain the unknown mean zonal
337 velocity U. In order to find U we substitute Fourier series (41) and (42) in the zonal
338 momentum balance equation (30). After some manipulation we obtain:

$$\tau_0 = \frac{8 f_0}{3 L_x} \sum_n n(a_n d_n - b_n c_n) + \frac{4\beta\, k_0 H}{\pi} \quad . \tag{49}$$

339 The method of solution to obtain U is presented in the Appendix.

340 The zonal flow is perturbed by the presence of topography and diffusion of QGPV. In the
341 case of a flat bottom, i.e. $c_n = d_n = 0$ the motion is unperturbed, since $S_0^{(n)} = S_1^{(n)} = S_2^{(n)} = 0$
342 (see (A4-A6)).

343 This analytical solution is possible because only a single meridional component of the
344 bottom topography B is retained. In the case of a more general expression of B it would be
345 much more difficult to obtain an analytical solution due to greatly increased mathematical
346 complexity.

347 The expressions for the unknowns a_n, b_n and U in equations (47-49) constitute an ana-
348 lytical solution for equation (23). There is no truncation error, since only the Fourier modes

represented in the bottom topography contribute. Note, that as long as the modulus of the amplitudes, c_n, d_n of the Fourier topographic modes are finite, then

$$\lim_{n\to\infty} a_n = \lim_{n\to\infty} b_n = 0 \ . \tag{50}$$

We evaluate the solution for a number of cases with different topography and different k_0 using parameter values relevant to the Southern Ocean: channel length $L_x = 4 \cdot 10^6$m and width 10^6m; reference depth $5 \cdot 10^3$m; Coriolis parameter $f_0 = -10^{-4}\mathrm{s}^{-1}$ and $\beta = 1.4 \cdot 10^{-11} m^{-1} s^{-1}$; and $\tau_0 = 10^{-4} m^2 s^{-2}$. We illustrate the streamfunction for three cases: case 1 specifies the topography as $c_3 = 300m$; case 2 specifies $c_1 = 300m$ and $d_1 = 300m$; case 3 specifies $c_2 = 300m$; $d_5 = 300m$ (see Figs. 2-4). Here and later the topographic Fourier coefficients whose values are not explicitly stated are set to zero.

All cases demonstrate eastward mean flow, with streamlines deflected by topographic features (see Figs. 2-4). In these cases the bottom topography and coefficient k_0 vary. Because they obstruct the flow, the topographic features (both the amplitude and length in the zonal direction) substantially affect the net zonal volume transport (Figs. 5-7, upper panels). The streamfunctions for given topography look similar for different coefficients, but not the total zonal transport, which decreases linearly from the case with $k_0 = 0$ to the highest allowed coefficient. As we demonstrate above, the coefficient k_0 must be positive and according to the kinetic energy balance (34) should be less than $k_{max} = \pi\tau_0/(4\beta H)$, since

$$\{E, \tau\} - \{E, \beta\} > 0 \ . \tag{51}$$

Under our selected parameters, $\pi\tau_0/(4\beta H) = 1.12 \cdot 10^3 m^2 s^{-1}$. However, our solutions demonstrate that the actual maximum value k_{max}^{eff} is less than this, i.e.

$$k_{max}^{eff} < k_{max} = \pi\tau_0/(4\beta H) \tag{52}$$

(see the middle panels in each Fig. 5-7). This is because k_{max}^{eff} depends not only on (51) but on the other terms on the RHS of (34) as well.

Under prescribed topography the maximum transport corresponds to $k_0 = 0$, which varies substantially (depending on topography). The highest transports are 300.5 Sv, 445.0 Sv, and 115.0 Sv in cases 1-3, respectively.

Being under the same external forcing (wind stress) the difference in transport occurs because of different bottom topography in these cases. The main momentum sink is the topographic form stress. This term strongly depends on the amplitudes and wavenumbers of the non-zero Fourier modes making up the topography. In order to quantify this dependence we introduce a new integral measure D of the roughness of the topography (r.m.s. of $(\partial B/\partial x)$):

$$D = \sqrt{\frac{1}{LL_x}\int_0^L \int_0^{L_x} (\frac{\partial B}{\partial x})^2 dxdy} \ . \tag{53}$$

Substituting (22) and (42) into (53) with an appropriate Fourier transformation we obtain:

$$D = \frac{\pi}{L_x}\sqrt{\sum_n (n^2(c_n^2 + d_n^2))} \ . \tag{54}$$

This integral scale of roughness is dimensionless and depends on the mode index n and the amplitude of the topography c_n, d_n. In Fig. 8 we plot points representing our calculations of transport for the same wind stress ($\tau_0 = 10^{-4}\mathrm{m}^2/\mathrm{s}^2$) and $k_0 = 0$, but for the various realizations of bottom topography and a fitting curve which is seen to resemble a hyperbola. If $D < 3 \cdot 10^{-4}$ there is a large variation of transport for a small variation of D. Small values of D correspond to low amplitudes of topography together with small mode index n (i.e. smooth topography). When $D > 3 \cdot 10^{-4}$ there is an approximately linear relation between transport and D.

All the terms on the RHS of equation (34) are positive (Figs. 5-7, middle panels) and contribute to balancing the source of kinetic energy ($\{E, \tau\}$). When $k_0 = 0$ there is a balance between generation of kinetic energy by wind stress and dissipation by bottom friction, i.e. $\{E, \tau\} = \{E, \epsilon\}$.

For small values of k_0, the bottom friction dominates the other terms. However with increasing k_0 the terms $\{E, h\}$ and $\{E, \beta\}$ increase, representing dissipation linked with

topography and the sink due to topographic form stress, respectively. These provide a substantial contribution to balancing the wind stress term. In all cases, the term $\{E, k\}$, representing dissipation by QGPV mixing remains small. $\{E, k\}$ is not directly linked with topography in contrast to $\{E, h\}$. The highest values of kinetic energy, E, and its components E_U and E_V occur when $k_0 = 0$, and kinetic energy decreases with increasing k_0 (see Figs. 5-7, lower panels). The component E_U may be higher than E_V (cases 1 and 2) or lower (case 3) depending on the details of the bottom topography.

Increasing wind stress leads to increasing zonal transport (see Fig. 9). In case 3 for $k_0 = 0$ a fivefold increase in wind stress amplitude $\tau_0 = 5 \cdot 10^{-4}\mathrm{m}^2/\mathrm{s}^2$ results in a factor 3 increase in transport from 115.0 Sv to 338.3 Sv. Note however that the transport does not increase linearly with increasing wind stress: the sensitivity reduces by a factor 2 from $\tau_0 = 1.10^{-4}\mathrm{m}^2/\mathrm{s}^2$ to $\tau_0 = 5.10^{-4}\mathrm{m}^2/\mathrm{s}^2$. Note, that this reducing sensitivity of the transport for high values of wind stress does not relate to eddy activity (recall we are considering the case $k_0 = 0$). Constantinou and Young (2017) and Constantinou (2018) found barotropic eddy saturation, i.e. insensitivity of the transport to wind forcing in QG flow in a barotropic configuration. On the other hand Munday *et al.* (2013) demonstrated eddy saturation in a three dimensional baroclinic setting using an ocean-only general circulation model. It would be interesting to verify eddy saturation in our model with parameterized eddies. However the transport strongly depends on the value of k_0 (Fig. 9). It would take additional effort to find the best-fitting coefficient k_0 for each wind stress. One approach would be to perform eddy resolving GCM experiments with given wind stress. Based on values of transport taken from these eddy resolving experiments, we could use the relationship between transport and k_0 (as in Fig. 9) to find the most realistic value of k_0 for each wind stress and then verify eddy saturation in the parameterized model.

5. Discussion and Conclusions

Mesoscale eddy parameterization is an important problem of physical oceanography helping to understand the dynamics of interactions of eddies with the mean flow. Moreover, even state of the art high resolution $\frac{1}{12}$ degree global models do not resolve mesoscale eddies in high latitudes.

There are various approaches to the problem of eddy parameterization. This study focuses on parameterization of eddy QGPV fluxes. PV and QGPV are conserved variables, which allows use of a diffusion type of parameterization, contrary to momentum, which is not conserved and therefore a diffusive parameterization is unsuitable in this case.

Whether or not the effective coefficient of potential vorticity diffusion is positive represents the principal question in studies of mesoscale eddy parameterization (Welander 1973, Marshall 1981). If the coefficient is of negative sign a diffusive parameterization cannot be used, since it would be both mathematically and physically incorrect. The sign of this coefficient in a zonal barotropic channel is the topic of the present paper. We have demonstrated that if transient eddies are adequately described as effective PV diffusion, then the mean PV diffusivity over the domain k_0 must be positive in eastward flows. This result comes out of the balance of the zonal momentum and kinetic energy: because of the parameterization, a new term appears in these equations with the physical sense of a topographic form stress for unresolved scales. The main zonal momentum balance is between wind stress (the LHS in (30)), topographic form stress exerted by the mean flow, and topographic form stress exerted by parameterized eddies.

The integral constraint on meridional fluxes of eddy QGPV known as the theorem of Bretherton in the case of a flat bottom channel is generalized for barotropic zonal flow under variable bottom relief. This expression allows us to provide a clear physical sense for the $\beta\, k$ term, as a topographic form stress exerted by parameterized eddies.

We introduce a new integral measure D of the roughness of the bottom topography, which is the r.m.s. of topographic slope. The best fitting curve representing the relationship

between zonal transport and D is of hyperbolic type with a large increase of the transport when D is small and decreasing, and a small decrease when D is large and increasing (Fig. 8).

In the kinetic energy balance, the only positive contribution comes from the wind stress $\{E, \tau\}$, which is balanced by eddy diffusion of potential vorticity $\{E, k\}$, eddy diffusion of QGPV linked with topography $\{E, h\}$, bottom dissipation $\{E, \epsilon\}$ and a sink of energy due to topographic form stress by parameterized eddies, i.e. $\{E, \beta\}$. This correctly explains the mechanism of flow deceleration by eddies associated with non zero bottom topography and it corresponds to downgradient QGPV eddy fluxes in eastward flow. Note that the topographic form stress is the main mechanism balancing the wind stress in the Antarctic Circumpolar Current (Munk and Palmen 1951; McWilliams, *et al.* 1978; Ivchenko *et al.* 1996; Stevens and Ivchenko 1997; Ivchenko *et al.* 2008). Provided the diffusion parameterization of eddy PV fluxes holds (i.e. provided eq. (9) is valid) then the deceleration mechanism of topographic form stress ensures $k_0 > 0$ for eastward (ACC-like) flows. Another result of our study is that k_0 is also constrained to be less than $k_{max} = (\pi\tau_0/(4\beta H))$, because $\{E, \tau\} - \{E, \beta\}$ must be positive (equation (51)). However, for any given choice of the prescribed wind stress and other geometrical and geophysical parameters k_0 is further constrained (i.e. $k_0 < k_{max}^{eff} < k_{max}$). In the cases considered we found $k_{max} < \pi\tau_0/(4\beta H) = 1.12 \cdot 10^3 m^2/s$. The individual values of k_{max}^{eff} were $4.7 \cdot 10^2 m^2/s$, $8.5 \cdot 10^2 m^2/s$, and $2.1 \cdot 10^2 m^2/s$ (for cases 1, 2 and 3), respectively (see middle panels of Figs. 5, 6 and 7).

Only modes represented in the bottom topography contribute to the amplitude of the streamfunction a_n and b_n (see (47)-(48)). Since the modulus of the amplitudes c_n, d_n of the Fourier topographic modes are finite, and $\lim_{n\to\infty} a_n = \lim_{n\to\infty} b_n = 0$ one can interpret this as a diminishing contribution of high frequency modes in topography to mean flow and topographic form stress. This agrees with numerical experiments by Treguier and McWilliams (1990), where they demonstrated that an isolated bottom topography feature of large spatial scale in the path of the ACC generates form stress more efficiently than ran-

domly distributed small-scale topography with the same r.m.s. height. They also noted that the domain-averaged topographic form stress is dominated by the contribution from large scale topography. The authors used a baroclinic QG model, however it is plausible that a barotropic model would produce qualitatively similar results regarding the influence of bottom topography. Note also, that the eddy field in our model would be damped ($k_0 \to 0$) in the case where $\beta \to 0$, since $k_{max} \to 0$.

Constantinou and Young (2017) demonstrated an "eddy saturation" regime, i.e. insensitivity of the zonal transport to large changes in the wind stress (provided the wind stress is over a threshold value), in a barotropic configuration. To study "eddy saturation" in our model we need to choose a value of k_0 for each type of topography, since the zonal transport depends strongly on k_0. In this context, the appropriate k_0 could be estimated using eddy resolving GCM experiments. For a given wind stress eddy resolving model experiments can be used to evaluate the associated transport and the relationship between transport and k_0 (similar to Fig. 9) can then be used to obtain an appropriate k_0. However this is beyond the scope of the present paper.

In summary, our study demonstrates conclusively that if QGPV diffusion is a good approximation, then the mean QGPV diffusivity must be positive. Our results will contribute to further understanding and parameterization of the effects of mesoscale eddies in more realistic ocean and climate models in the future.

Acknowledgments. We thank two anonymous Reviewers for their substantial efforts in reviewing our paper. Their comments were extremely helpful and led to a much improved manuscript. VOI acknowledges the support of the University of Southampton and the National Oceanography Centre. VBZ was supported by the Russian Science Foundation, Grant number 17-77-30001. BS was supported by National Capability funding from the UK Natural Environment Research Council.

Appendix

In developing solutions for a_n and b_n (47-48) the new parameters introduced are listed

here:

$$R_0^{(n)} = -N^{(n)} - \frac{1}{N^{(n)}}\beta^{\,2}(\frac{2\pi}{L_x})^2 n^2 \quad ,(A1)$$

$$R_1^{(n)} = \frac{2}{N^{(n)}} M^{(n)} \beta\,(\frac{2\pi}{L_x}) n \quad ,(A2)$$

$$R_2^{(n)} = -\frac{1}{N^{(n)}} M^{(n)\,2} \quad ,(A3)$$

$$S_0^{(n)} = -\frac{1}{N^{(n)}} d_n\, k_0 \frac{f_0}{H}(\frac{2\pi}{L_x})^3 n^3 \beta - c_n\, k_0 \frac{f_0}{H}(\frac{2\pi}{L_x})^2 n^2 \quad ,(A4)$$

$$S_1^{(n)} = \frac{1}{N^{(n)}} c_n \frac{f_0}{H}(\frac{2\pi}{L_x})^2 \beta\, n^2 + \frac{1}{N^{(n)}} d_n\, k_0 \frac{f_0}{H}(\frac{2\pi}{L_x})^2 M^{(n)}\, n^2 - d_n \frac{f_0}{H}(\frac{2\pi}{L_x}) n \quad ,(A5)$$

$$S_2^{(n)} = -\frac{1}{N^{(n)}} c_n \frac{f_0}{H} M^{(n)} (\frac{2\pi}{L_x}) n \quad .(A6)$$

Equations (47), (48) and (49) together constitute the desired analytic solution. However because of the mathematical complexity we are unable to obtain explicit solutions for U in terms of the external parameters. Instead we apply an inverse solution method. We seek values of U which are consistent with the specified windstress τ_0 (for example $10^{-4} m^2/s^2$ in the standard case). We make an initial guess of U, substitute this in eq. (47) and (48) to give initial estimates of a_n and b_n. These estimates are then substituted in eq. (49) to obtain a corresponding value of τ_0. In general the initial guess does not yield the desired value of τ_0. We therefore increase/decrease the guessed value of U and repeat the procedure until we find the value of U which yields the desired value of τ_0 (to within 0.1%) (see Fig. 10). In order to determine the relationship between k_0 and U for a given windstress, the above procedure is repeated for a variety of choices of k_0.

REFERENCES

Abernathey, R., D. Ferreira, and A. Klocker, 2013: Diagnostics of isopycnal mixing in a circumpolar channel. *Ocean Modelling*, **72**, 1-16.

Bachman, S., and B. Fox-Kemper, 2013: Eddy parameterization challenge suite 1: Eady spindown. *Ocean Modelling*, **64**, 12-28.

Birner, T., D.W.J. Thompson, and T.G. Sheperd, 2013: Up-gradient eddy fluxes of potential vorticity near the subtropical jet. *Geophys. Res. Lett.*, **40**, 5988-5993.

Bretherton, F. S., 1966: Critical layer instability in baroclinic flows. *Quart. J. Roy. Met. Soc.*, **92**, 325-334.

Carnevale, G.F., and J.S. Frederiksen, 1987: Nonlinear stability and statistical mechanics of flow over topography. *J. Fluid. Mech.*, **175**, 157-181.

Constantinou, N.C., 2018: A barotropic model of eddy saturation. *J. Phys. Oceanogr.*, **48**, 397-411.

Constantinou, N.C., and W.R. Young, 2017: Beta-plane turbulence above monoscale topography. *J. Fluid. Mech.*, **827**, 415-447.

Charney, J.G., J. Shukla, and K.C. Mo, 1981: Comparison of a barotropic blocking theory with observation. *J. Atmos. Sci.*, **38**, 762-779.

Dritschel, D.G., and M.E. McIntyre, 2008: Multiple jets as PV staircases: the Philips effect and the resilience of eddy-transport barriers. *J. Atmos. Sci.*, **65**, 855-874.

Eden, C., 2010: Parameterising meso-scale eddy momentum fluxes based on potential vorticity mixing and a gauge term. *Ocean Modelling*, **32**, 58-71.

Fox-Kemper, B., R. Ferrari, and J. Pedlosky, 2003: On the indeterminacy of rotational and divergent eddy fluxes. *J. Phys. Oceanogr.*, **33**, 478-483.

Gent, P.R., and J.C. McWilliams, 1990: Isopycnal mixing in ocean circulation models. *J. Phys. Oceanogr.*, **20**, 150-155.

Green, J. S. A., 1970: Transfer properties of the large-scale eddies and the general circulation of the atmosphere. *Quart. J. Roy. Met. Soc.*, **96**, 157-185.

Ivchenko, V. O., 1984: Parameterization of the eddy fluxes of the quasi-geostrophic potential vorticity in zonal flows. *Doklady Acad. Nauk USSR*, **277**, 972–976.

Ivchenko, V. O., 1987: Influence of bottom topography on the eddy transfer coefficient. *Izvestiya Acad. Nauk USSR. Atmosphere and Ocean Physics*, **23**, 200-208.

Ivchenko, V. O., S. Danilov, and D. Olbers, 2008: Eddies in numerical models of the Southern Ocean. Chapter in monograph:'Ocean modeling in an eddying regime' (Eds. M. Hecht and H. Hasumi), AGU, 177-198.

Ivchenko, V. O., K. J. Richards, and D. P. Stevens, 1996: The dynamics of the Antarctic Circumpolar Current. *J. Phys. Oceanogr.*, **26**, 753-774.

Ivchenko, V. O., K. J. Richards, B. Sinha, and J-O. Wolff, 1997: Parameterization of mesoscale eddy fluxes in zonal ocean flows. *J. Mar. Res.*, **55**, 1127-1162.

Ivchenko, V. O., B. Sinha, V. B. Zalesny, R. Marsh, and A. T. Blaker, 2013: Influence of bottom topography on integral constraints in zonal flows with parameterized potential vorticity fluxes. *J. Phys. Oceanogr.*, **43**, 311-323.

Ivchenko, V. O., S. Danilov, B. Sinha, and J. Schroeter, 2014(a): Integral constraints for momentum and energy in zonal flows with parameterized potential vorticity fluxes: governing parameters. *J. Phys. Oceanogr.*, **44**, 922-943.

Ivchenko V.O., S. Danilov, and J. Shroeter, 2014(b): Comparison of the effect of parameterized eddy fluxes of thickness and potential vorticity. *J. Phys. Oceanogr.*, **44**, No.9, 2470-2484.

564 Kamenkovich, V. M., M. N. Koshlyakov, and A. S. Monin, 1986: Synoptic eddies in the
565 ocean, *D.Reidel Publishing Company, Dordrecht, Holland*, 433 pp.

566 Killworth, P. D., 1997: On the parameterization of eddy transfer. Part 1. Theory. *J. Mar.*
567 *Res.*, **55**, 1171-1197.

568 Maddison, J.R., D.P. Marshall, and J. Shipton, 2015: On the dynamical influence of ocean
569 eddy potential vorticity fluxes. *Ocean Modelling*, **92**, 169-182.

570 Mak., J, J.R. Maddison, and D.P. Marshall, 2016: A new gauge-invariant method for diag-
571 nosting eddy diffusivities. *Ocean Modelling*, **104**, 252-268.

572 Marshall, J.C., 1981: On the parameterization of geostrophic eddies in the ocean. *J. Phys.*
573 *Oceanogr.*, **11**, 257-271.

574 Marshall, D. P., and A. J. Adcroft, 2010: Parameterization of ocean eddies: Potential
575 vorticity mixing, energetics and Arnold's first stability theorem. *Ocean Modelling*, **32**,
576 188-204.

577 Marshall, D. P., J. R. Maddison, and P. S. Berloff, 2012: A framework for parameterizing
578 eddy potential vorticity fluxes. *J. Phys. Oceanogr.*, **42**, 539-557.

579 McWilliams, J. C., 2008: The nature and consequences of oceanic eddies. Chapter in mono-
580 graph: 'Ocean modeling in an eddying regime' (Eds. M. Hecht and H. Hasumi), AGU,
581 5-15.

582 McWilliams, J.C. and Chow J.S. 1981: Equilibrium geostrophic turbulemce. 1. A reference
583 solution in a beta plane channell. Isopycnal mixing in ocean circulation models. *J. Phys.*
584 *Oceanogr.*, **11**, 921-949.

585 McWilliams, J. C., W. R. Holland, and J. S. Chow, 1978: A description of numerical Antarc-
586 tic Circumpolar Currents. *Dyn. Atmos. Oceans.*, **2**, 213-291.

587 Munday, D.R., H.L. Johnson, and D.P. Marshall, 2013: Eddy saturation of equilibrated
588 circumpolar currents. *J. Phys. Oceanogr.*, **43**, 507-532.

589 Munk, W.H., and E. Palmén, 1951: Note on the dynamics of the Antarctic Circumpolar
590 Current, *Tellus*, **3**, 53-55.

591 Olbers, D., 2005: On the role of eddy mixing in the transport of zonal ocean currents.
592 *Marine turbulence. Theories, Observations, and Models.* Eds. H. Baumert, J. Simpson,
593 and J. Sündermann. Cambridge Univ. Press, 630 pp.

594 Olbers, D., J. Wolff, and C. Voelker. 2000: Eddy fluxes and second-order moment bal-
595 ances for nonhomogeneous quasigeostrophic turbulence in wind-driven zonal flows. *J. Phys.*
596 *Oceanogr.*, **30**, 1645-1668.

597 Rhines, P.B., and W.R. Young, 1982: Homogenization of potential vorticity in planetary
598 gyres. *J. Fluid. Mech.*, **122**, 347-367.

599 Ringler, T., and P. Gent, 2011: An eddy closure for potential vorticity. *Ocean Modelling*,
600 **39**, 125-134.

601 Sinha, B., 1993: The influence of mesoscale eddies and topography on Southern Ocean Flow.
602 Ph.D. Thesis, Southampton University, 197 pp.

603 Smith, D.M., S. Cusack, A.W. Colman, C.K. Folland, G.R. Harris, and J.M. Murphy, 2007:
604 Improved surface temperature prediction for the Coming Decade from a Global Climate
605 Model. *Science*, **317**, 5839, pp.796-799.

606 Stevens, D. P. and V. O. Ivchenko, 1997: The zonal momentum balance in an eddy–resolving
607 general–circulation model of the Southern Ocean. *Quart. J. Roy. Met. Soc.*, **123**, 929-951.

608 Treguier, A. M., I. M. Held, and V. D. Larichev, 1997: Parameterization of quasigeostrophic
609 eddies in primitive equation ocean models. *J. Phys. Oceanogr.*, **27**, 567-580.

610 Treguier, A. M., and J. C. McWilliams, 1990: Topographic influences on wind-driven, strat-
611 ified flow in a β-plane channel: an idealized model for the Antarctic Circumpolar Current.
612 *J. Phys. Oceanogr.*, **20**, 321-343.

613 Vallis, G.K., 2006: Atmospheric and oceanic fluid dynamics. Fundamentals and large-scale
614 circulation. Cambridge Univ. Press, Cambridge, 745 pp.

615 Wardle R., and J. Marshall, 2000: Representation of eddies in primitive equation models by
616 a PV flux. *J. Phys. Oceanogr.*, **30**, 2481-2503.

617 Welander, P., 1973: Lateral friction in the ocean as an effect of potential vorticity mixing.
618 *Geophys. Fluid Dyn.*, **5**, 173-189.

619 Wolff, J.-O., E. Maier-Reimer and D. J. Olbers, 1991: Wind-driven flow over topography in
620 a zonal β-plane channel: A quasigeostrophic model of the Antractic Circumpolar Current.
621 *J. Phys. Oceanogr.*, **21**, 236-264.

622 Wood, R.B., and M.E. McIntyre, 2010: A general theorem on angular-momentum changes
623 due to potential vorticity mixing and on potential-energy changes due to buoyancy mixing.
624 *J. Atmos. Sci.*, **67**, 1261-1274.

625 Wunsch, C., and D. Stammer 1995: The global frequency-wavenumber spectrum of oceanic
626 variability estimated from TOPEX/POSEIDON altimetric measurements. *J. Geophys.*
627 *Res.*, **100**, 24895-24910.

List of Figures

1 Meridional profile of the QGPV diffusion coefficient k normalized by k_0. 32

2 Upper panel: Bottom topography (m) represented by $c_3 = 300m$ (case 1). Here and in subsequent Figures the topographic Fourier coefficients whose values are not explicitly stated are set to zero. 2nd to 4th panels: streamfunction Ψ, times reference depth H (Sv), with $k_0 = 0, 200m^2/s$ and $400m^2/s$, respectively. 33

3 Upper panel: Bottom topography (m) represented by $c_1 = 300m$ and $d_1 = 300m$ (case 2). 2nd to 4th panels: streamfunction Ψ, times reference depth H (Sv), with $k_0 = 0, 400m^2/s$ and $800m^2/s$, respectively. 34

4 Upper panel: Bottom topography (m) represented by $c_2 = 300m$ and $d_5 = 300m$ (case 3). 2nd to 4th panels: streamfunction Ψ, times reference depth H (Sv), with $k_0 = 0, 100m^2/s$ and $200m^2/s$, respectively. 35

5 Upper panel: zonal transport (Sv) as a function of k_0 (m^2/s). Middle panel: components of the domain averaged energy budget $\{E, \tau\}$, $\{E, \beta\}$, $\{E, k\}$, $\{E, h\}$ and $\{E, \epsilon\}$ (m^2/s^3) as functions of k_0 (m^2/s). Bottom panel: domain averaged kinetic energy E_U and E_V (m^2/s^2) as functions of k_0. All panels represent case 1: bottom topography $c_3 = 300m$. 36

6 Upper panel: zonal transport (Sv) as a function of k_0 (m^2/s). Middle panel: components of the domain averaged energy budget $\{E, \tau\}$, $\{E, \beta\}$, $\{E, k\}$, $\{E, h\}$ and $\{E, \epsilon\}$ (m^2/s^3) as functions of k_0 (m^2/s). Bottom panel: domain averaged kinetic energy E_U and E_V (m^2/s^2) as functions of k_0. All panels represent case 2: bottom topography $c_1 = 300m$, $d_1 = 300m$. 37

7 Upper panel: zonal transport (Sv) as a function of k_0 (m^2/s). Middle panel: components of the domain averaged energy budget $\{E, \tau\}$, $\{E, \beta\}$, $\{E, k\}$, $\{E, h\}$ and $\{E, \epsilon\}$ (m^2/s^3) as functions of k_0 (m^2/s). Bottom panel: domain averaged kinetic energy E_U and E_V (m^2/s^2) as functions of k_0. All panels represent case 3: bottom topography $c_2 = 300m$, $d_5 = 300m$. 38

8 Scatter-plot of zonal transport (Sv) versus parameter of topographic roughness D for various realizations of bottom topography. The fitting curve is based on a 7-th order polynomial approximation. 39

9 Zonal transport (Sv) as a function of k_0 (m^2/s) for various wind stress. Case 3: bottom topography $c_2 = 300m$, $d_5 = 300m$. 40

10 Relationship between the mean zonal velocity U and the wind stress amplitude τ_o. Case 2: bottom topography $c_1 = 300m$, $d_1 = 300m$. 41

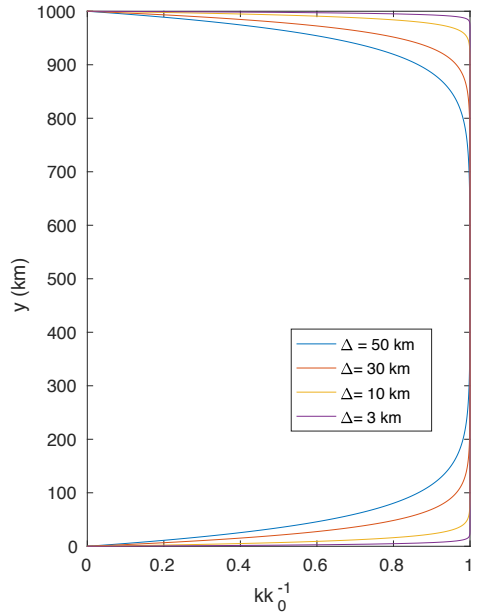

FIG. 1. Meridional profile of the QGPV diffusion coefficient k normalized by k_0.

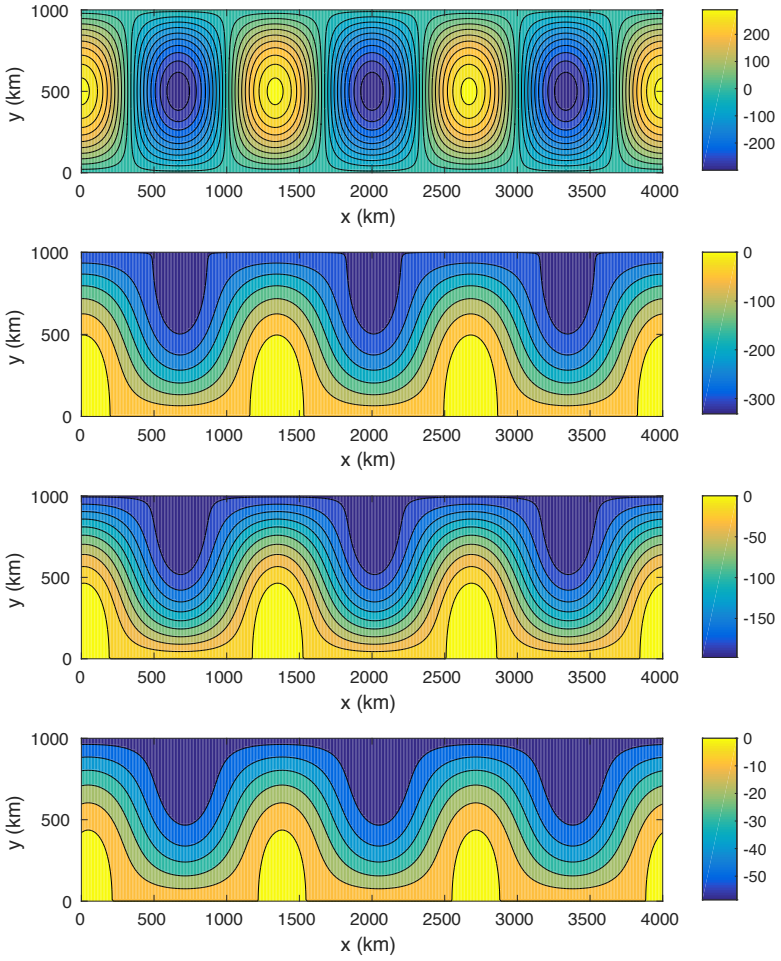

FIG. 2. Upper panel: Bottom topography (m) represented by $c_3 = 300m$ (case 1). Here and in subsequent Figures the topographic Fourier coefficients whose values are not explicitly stated are set to zero. 2nd to 4th panels: streamfunction Ψ, times reference depth H (Sv), with $k_0 = 0, 200m^2/s$ and $400m^2/s$, respectively.

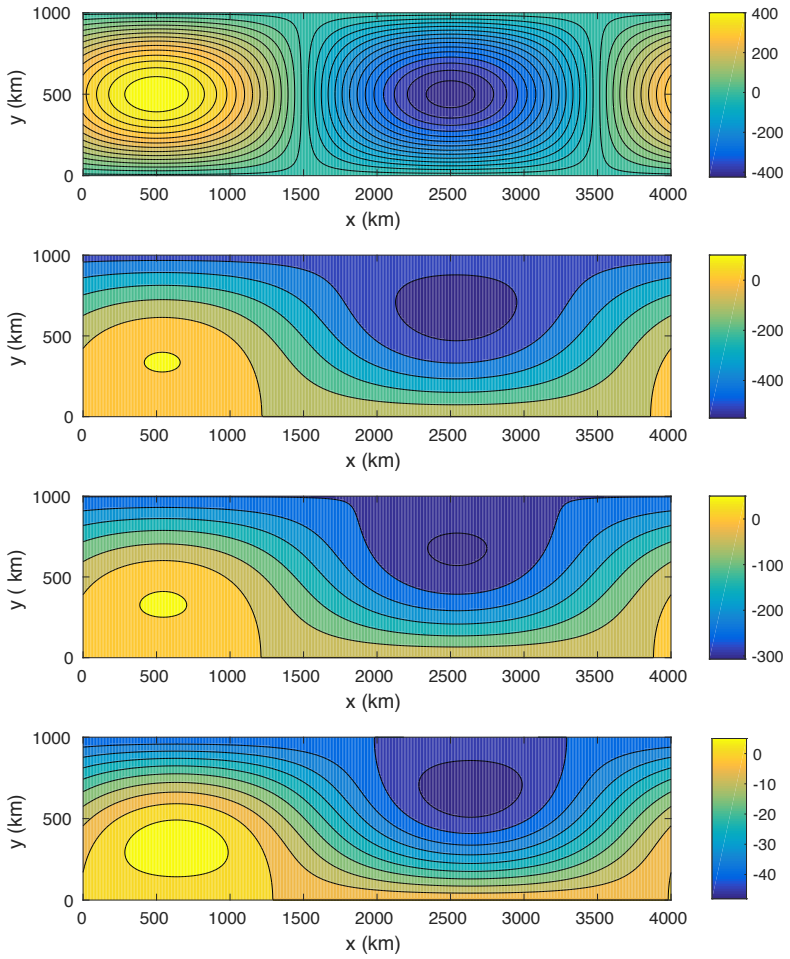

FIG. 3. Upper panel: Bottom topography (m) represented by $c_1 = 300m$ and $d_1 = 300m$ (case 2). 2nd to 4th panels: streamfunction Ψ, times reference depth H (Sv), with $k_0 = 0, 400m^2/s$ and $800m^2/s$, respectively.

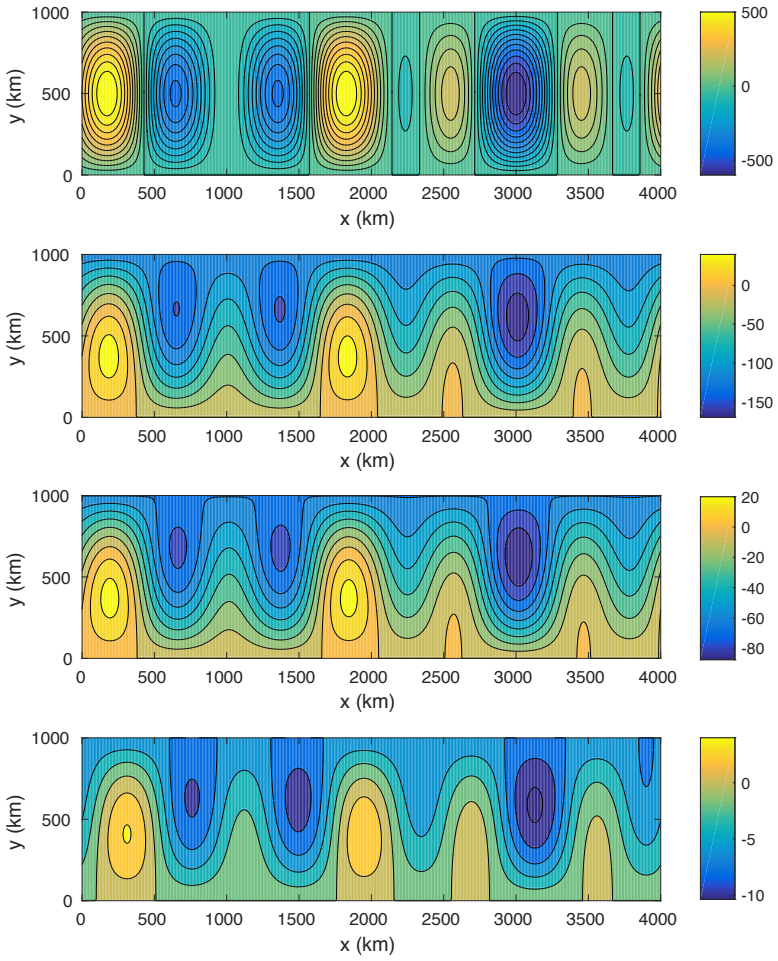

FIG. 4. Upper panel: Bottom topography (m) represented by $c_2 = 300m$ and $d_5 = 300m$ (case 3). 2nd to 4th panels: streamfunction Ψ, times reference depth H (Sv), with $k_0 = 0, 100m^2/s$ and $200m^2/s$, respectively.

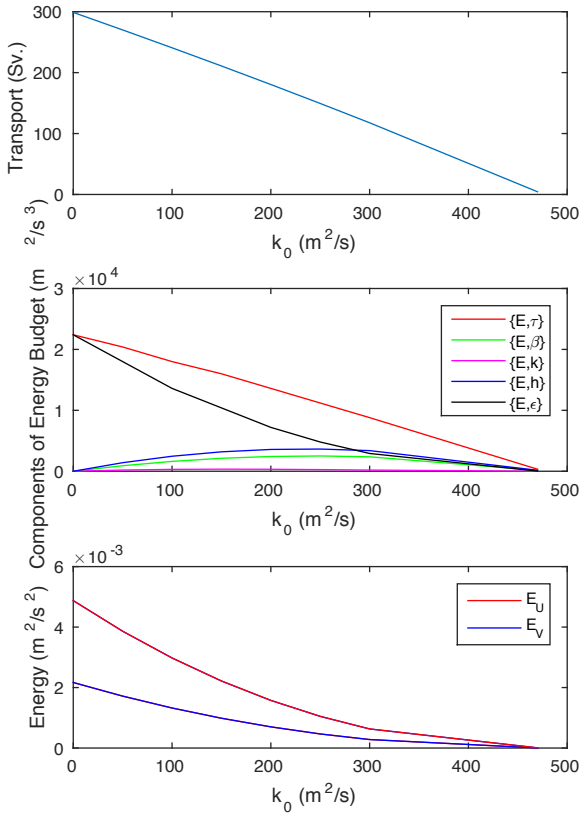

FIG. 5. Upper panel: zonal transport (Sv) as a function of k_0 (m^2/s). Middle panel: components of the domain averaged energy budget $\{E,\tau\}$, $\{E,\beta\}$, $\{E,k\}$, $\{E,h\}$ and $\{E,\epsilon\}$ (m^2/s^3) as functions of k_0 (m^2/s). Bottom panel: domain averaged kinetic energy E_U and E_V (m^2/s^2) as functions of k_0. All panels represent case 1: bottom topography $c_3 = 300m$.

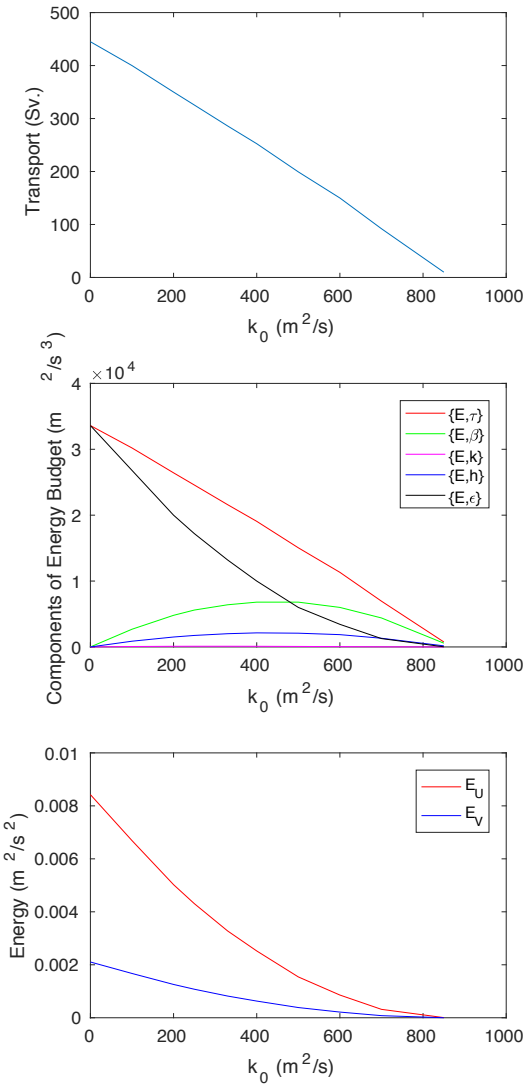

FIG. 6. Upper panel: zonal transport (Sv) as a function of k_0 (m^2/s). Middle panel: components of the domain averaged energy budget $\{E,\tau\}$, $\{E,\beta\}$, $\{E,k\}$, $\{E,h\}$ and $\{E,\epsilon\}$ (m^2/s^3) as functions of k_0 (m^2/s). Bottom panel: domain averaged kinetic energy E_U and E_V (m^2/s^2) as functions of k_0. All panels represent case 2: bottom topography $c_1 = 300m$, $d_1 = 300m$.

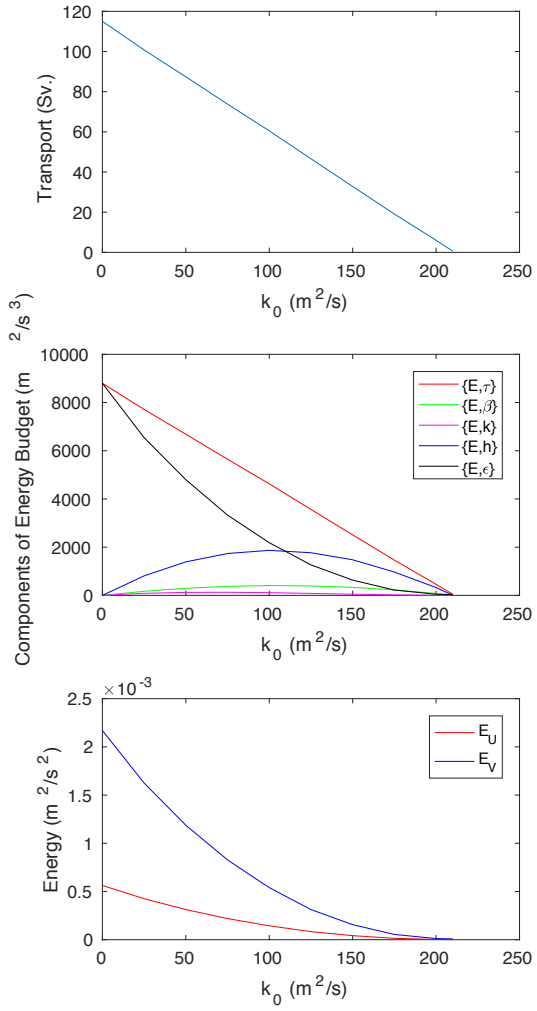

FIG. 7. Upper panel: zonal transport (Sv) as a function of k_0 (m^2/s). Middle panel: components of the domain averaged energy budget $\{E,\tau\}$, $\{E,\beta\}$, $\{E,k\}$, $\{E,h\}$ and $\{E,\epsilon\}$ (m^2/s^3) as functions of k_0 (m^2/s). Bottom panel: domain averaged kinetic energy E_U and E_V (m^2/s^2) as functions of k_0. All panels represent case 3: bottom topography $c_2 = 300m$, $d_5 = 300m$.

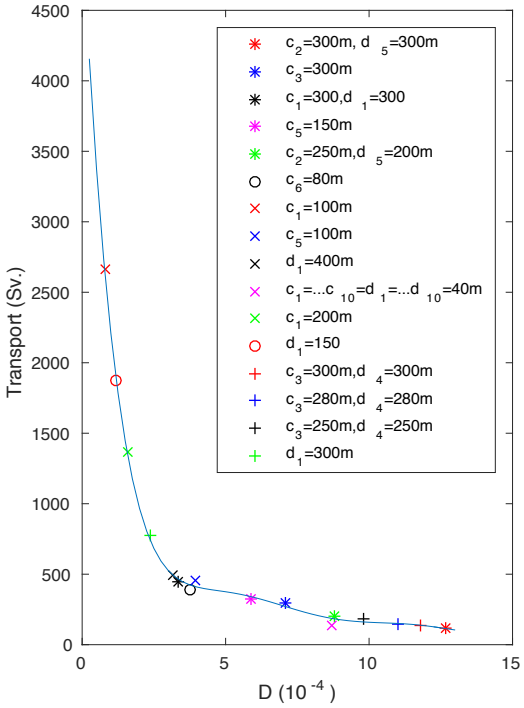

FIG. 8. Scatter-plot of zonal transport (Sv) versus parameter of topographic roughness D for various realizations of bottom topography. The fitting curve is based on a 7-th order polynomial approximation.

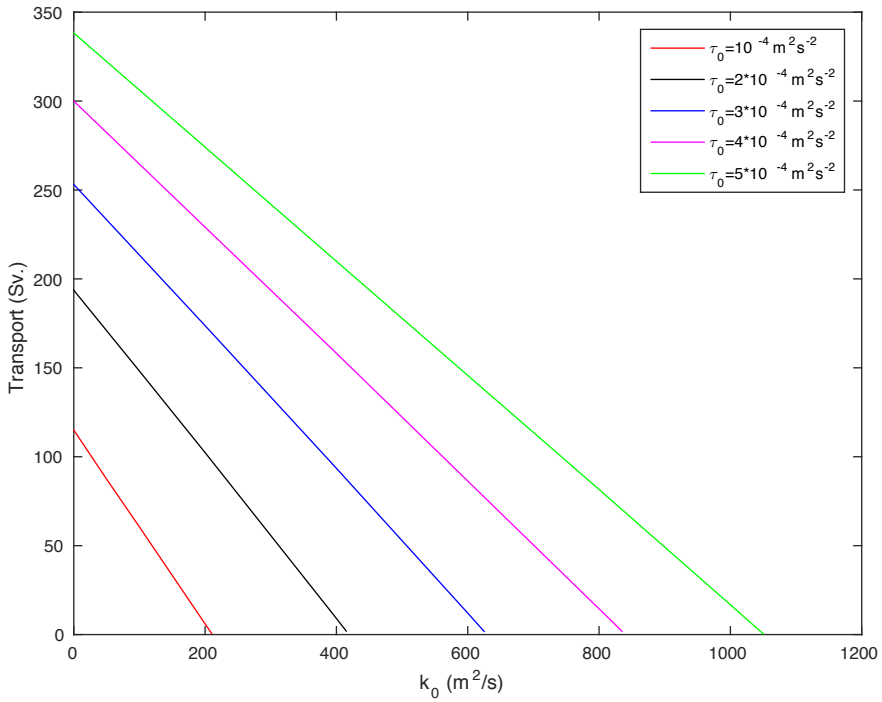

FIG. 9. Zonal transport (Sv) as a function of k_0 (m^2/s) for various wind stress. Case 3: bottom topography $c_2 = 300m$, $d_5 = 300m$.

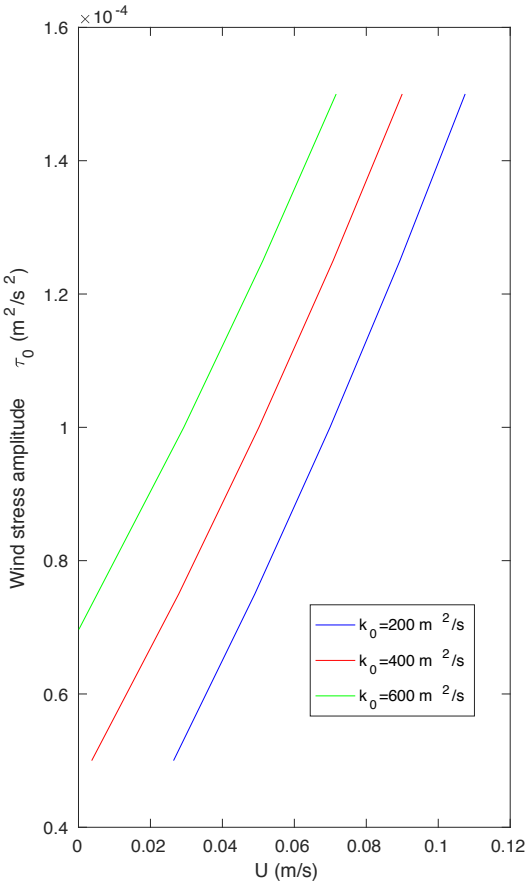

FIG. 10. Relationship between the mean zonal velocity U and the wind stress amplitude τ_o. Case 2: bottom topography $c_1 = 300m$, $d_1 = 300m$.